AJNR Am J Neuroradiol 21:1315–1319, August 2000

The Pterygopalatine Fossa: Postoperative MR Imaging Appearance

Ling-Ling Chan, June Chong, Ann M. Gillenwater, and Lawrence E. Ginsberg

BACKGROUND AND PURPOSE: **The pterygopalatine fossa (PPF) is an important anatomic location of the deep portion of the face. It is essential to review this area on both pre- and posttreatment studies of head and neck malignancies to assess local extent of disease or recurrence and perineural tumor spread. The purpose of this study was to review the postoperative appearance of the PPF on MR images.**

METHODS: **Imaging and clinical data of 10 patients who underwent surgical resection of tumor in which the PPF was violated at surgery were reviewed. Patients were included in the study if there was no imaging or clinical evidence of tumor in the PPF pre- or postoperatively. Postoperative MR studies were examined to assess the appearance of the PPF.**

RESULTS: **The PPF is consistently and persistently abnormal after surgical violation. There is loss of the normal T1 signal hyperintensity and abnormal, increased contrast enhancement, as seen on fat-suppressed T1-weighted images. These postoperative changes are strikingly similar to those of tumor involvement.**

CONCLUSION: **After surgical violation, the PPF will always appear abnormal on MR images, and the expected imaging findings must be recognized to avoid the misdiagnosis of tumor recurrence.**

The pterygopalatine fossa (PPF) is a critical neurovascular crossroad of the deep portion of the face and a common site for direct invasion and perineural spread of disease (1–3). Tumor involvement of the PPF has important treatment and prognostic implications (4–6). Hence, the PPF is an important area to review in head and neck imaging, both in the staging of newly diagnosed malignancies and follow-up imaging after treatment of disease. Much has been reported of the normal appearance of the PPF and its appearance after disease involvement (1–3, 7–13). How surgical violation of a disease-free PPF during head and neck surgery affects its postoperative MR imaging appearance has not been described. The purpose of this study was to review the postoperative appearance of the disease-free PPF on MR images so that it can be distinguished from disease.

Received November 17, 1999; accepted after revision January 31, 2000.

From the Departments of Diagnostic Radiology (L.-L.C, J.C., L.E.G.) and Head and Neck Surgery (A.M.G.), The University of Texas M. D. Anderson Cancer Center, Houston, Texas.

Presented at the Annual Meeting of the American Society of Head and Neck Radiology, San Diego, California, May 1999.

Address reprint requests to Lawrence E. Ginsberg, MD, Diagnostic Radiology, Box 57, The University of Texas M. D. Anderson Cancer Center, 1515 Holcombe Boulevard, Houston, TX 77030.

Methods

Eight men and two women (mean age, 53.7 years; age range, 46–70 years) were included in the study (Table). These patients satisfied the following inclusion criteria: 1) imaging evidence of absence of disease in the PPF before surgery; 2) documented surgical violation of the PPF during surgery; and 3) freedom from disease in the PPF at radiologic and clinical follow-up. The diagnoses of these patients included squamous cell carcinoma (five patients), adenoid cystic carcinoma (two patients), malignant melanoma (two patients), and malignant fibrous histiocytoma (one patient) (Table). The primary head and neck neoplasms involved the maxillary sinus (eight cases), hard palate (one case), and infratemporal fossa (two cases).

All patients had undergone either preoperative MR imaging (n = 8) or CT (n = 2) revealing an ipsilateral, normal, fat-containing PPF, which was confirmed at surgery. The hospital medical records were reviewed for any adjuvant radiation and chemotherapy that the patients received and their temporal relation to the imaging and surgery. For five patients, the preoperative MR scans were obtained after adjuvant radiation alone (n = 1), chemotherapy alone (n = 2), or both (n = 2) (Table). The other five patients also had a normal-appearing PFF on preoperative images obtained before radiation or chemotherapy, although for four patients, the postoperative MR scans were obtained after adjuvant radiotherapy.

Regular follow-up examinations of patients included CT or MR imaging or both to exclude tumor recurrence after surgical resection. Only the MR scans were examined for the appear-

TABLE: Patient data

Patient Age (yrs)/ Sex	Diagnosis and Site	Surgery	Postop MR Scans Obtained	Disease-free on MR	PPF (months) Clinically
55/M	Left maxillary sinus malignant fibrous histiocytoma	Radical maxillectomy orbital exenteration	4	26	27
63/M	Left maxillary sinus squamous cell carcinoma	Radical maxillectomy orbital exenteration	2	18	23
55/F	Left palate adenoid cystic carcinoma	Total maxillectomy	1	10	43
49/M	Left maxillary sinus adenoid cystic carcinoma	Suprastructure maxillectomy orbital exenteration	5	24	24
51/F	Right maxillary sinus squamous cell carcinoma	Radical maxillectomy orbital exenteration	3	10.5	11
70/M	Left maxillary sinus squamous cell carcinoma	Partial maxillectomy orbital exenteration	10	79	80
46/M	Right maxillary sinus metastatic melanoma	Total maxillectomy	9	21.5	22
48/M	Left infratemporal fossa squamous cell carcinoma	Partial maxillectomy orbital exenteration	4	13.5	14
54/M	Right maxillary sinus, infratemporal squamous cell carcinoma	Partial maxillectomy	5	14	14
46/M	Left maxillary sinus metastatic melanoma	Suprastructure maxillectomy orbital exenteration	4	6.5	7
Total			47	223	265

ance of the postoperative PPF. The scans were obtained on a 1.5-T (GE Signa; GE, Milwaukee, WI) MR imaging unit, using the head coil. The following sequences were obtained: conventional spin-echo T1-weighted (400–633/9–12 [TR/TE]), fast spin-echo T2-weighted (4000–5650/98–105), and contrast (gadolinium chelate)-enhanced, fat-suppressed T1-weighted (433–566/9–12) images. Other typical imaging parameters included 2 excitations, 3- to 5-mm-thick sections with 1- to 1.5-cm interslice gaps, a 256 × 192 matrix size, and a 16 × 16 or 18 × 18 cm field of view. The radiologic criteria for exclusion of tumor recurrence was stability relative to the baseline postoperative MR study, with no increase in width of the PPF, no interval development of a mass, and no imaging evidence of perineural tumor spread along the proximal course of the maxillary nerve.

All patients were clinically assessed to be free of disease recurrence in the PPF during the period of this study. Specifically, this included no progression of or new cranial neuropathy or clinical evidence of a new mass. The total number of postoperative MR scans and disease-free months during radiographic and clinical follow-up were recorded.

Results

All 10 PPFs that were violated during surgery for ipsilateral head and neck neoplasm appeared abnormal on postoperative MR images and remained abnormal in appearance on serial scans. The small neurovascular structures and fat signal normally found on images of the PPF were not seen on T1-weighted images (Fig 1A). The PPF was replaced by soft-tissue thickening of less than 10 mm ($n = 7$) or was contiguous with grafting material anterior to the PPF and occupying the orbital, maxillary, and/or infratemporal surgical defect ($n = 3$). The soft-tissue signal was generally hypointense or isointense to muscle on T1-weighted images, heterogeneous and mixed on T2-weighted images, and showed abnormal enhancement of varying degrees (Figs 1B–F and 2). These changes persisted in all cases, despite clinical absence of recurrent disease in the PPF (Figs 1E, F and 2). Specifically, there was no increase in the width of the postoperative PPF, and the degree of enhancement (allowing for differences in technique, windowing, etc) did not significantly change with time. The T1 and T2 signal intensities did not significantly change over time. There was no interval development of new masslike lesions or perineural extension to adjacent spaces.

All patients except one underwent postoperative MR imaging at least twice (range, 1–10 imaging sessions; mean, 4.7 imaging sessions) (Table). The patient who underwent postoperative MR imaging only once was included because serial CT and 43 months of follow-up revealed that she remained radiographically and clinically stable and free of disease recurrence in the PPF. The period from surgical violation of the PPF through the last MR imaging session that showed stability of findings in the PPF ranged from 6.5 to 79 months (mean, 22.3 months) in our patients. Clinical follow-up of 7 to 80 months (mean, 26.5 months) showed freedom of disease recurrence in the PPF (Table).

Discussion

The PPF is a pyramidal space located inferior to the orbital apex and posterior to the maxillary sinus. It contains the maxillary nerve (second division of the trigeminal nerve and its branches), the pterygopalatine ganglion, and terminal branches of the internal maxillary artery (3, 14–16). It is bound posteriorly by the pterygoid plates, medially by the palatine bone, and anteriorly by the maxillary bone. Laterally, it communicates with the infratemporal fossa via the pterygomaxillary fissure. It also connects with the nasal cavity medially via the sphenopalatine foramen, the orbit via the inferior orbital fissure, and intracranial space via the foramen rotundum. Posteriorly, the anterior opening of the vidian canal permits the entrance of the vidian nerve, which constitutes the preganglionic parasympathetic component of the pterygopalatine ganglion. Inferiorly, the descending pterygoid canal leads to the

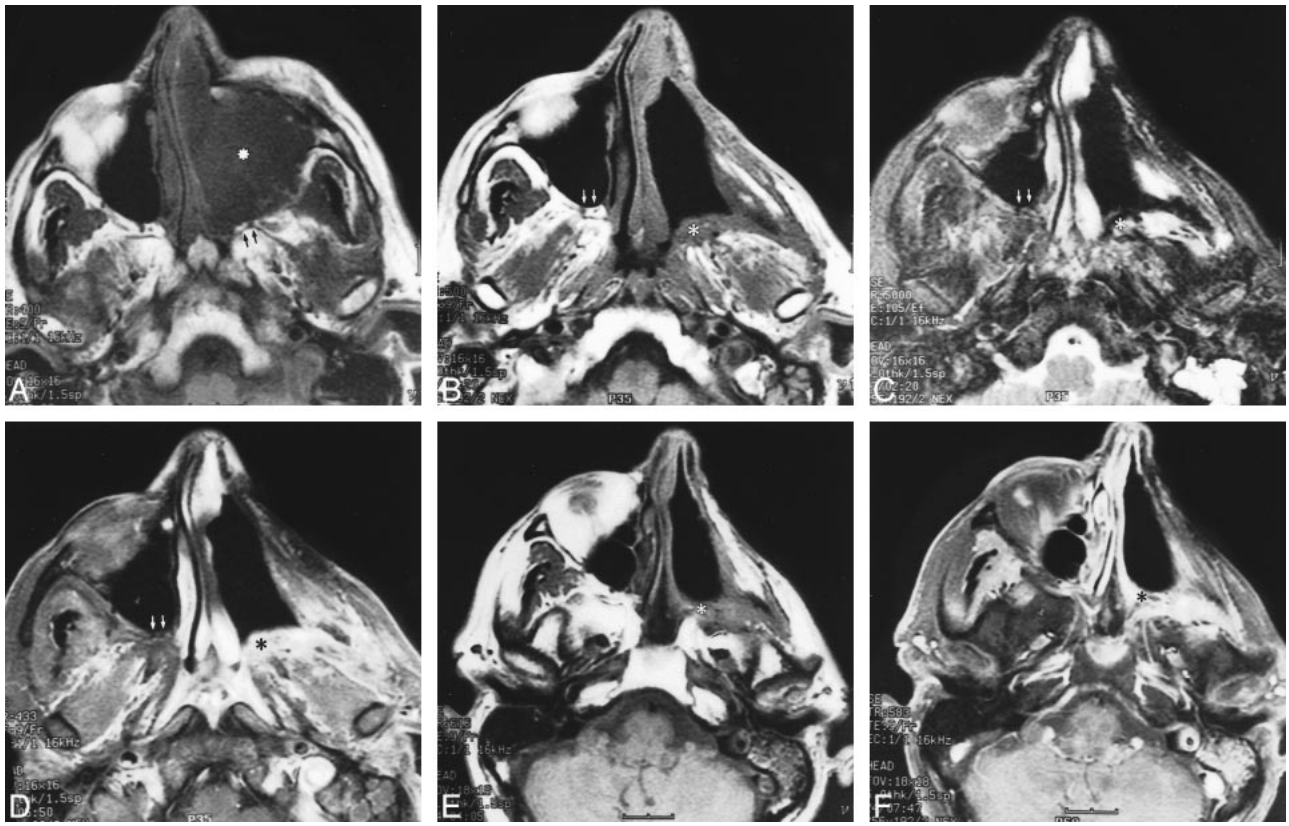

FIG 1. Axial MR images of a 55-year-old man with a left maxillary sinus malignant fibrous histiocytoma.

A, Preoperative unenhanced T1-weighted (400/9/2 [TR/TE/excitations]) image shows large tumor opacifying and expanding the left maxillary sinus (*asterisk*). Note the normal fat signal and neurovascular contents within the compressed left PPF (*arrows*).

B–D, Obtained 4 months after radical maxillectomy, T1-weighted (500/9/2) (*B*), T2-weighted (5000/105/2) (*C*), and contrast-enhanced fat-suppressed T1-weighted (433/9/2) (*D*) images show soft-tissue thickening in the left PPF (*asterisk*). This is isointense to muscle (*B*), has heterogeneous but generally hyperintense T2 signal (*C*), and enhances brightly (*D*). None of these changes are present in the normal, contralateral PPF (*arrows*).

E and *F,* Unenhanced T1-weighted (616/9/2) (*E*) and contrast-enhanced fat-suppressed T1-weighted (583/9/2) (*F*) images obtained 20 months after radical maxillectomy show persistent soft-tissue thickening (*E*) and excessive enhancement (*F*) in the left PPF (*asterisk*).

greater and lesser palatine foramina, which access the palate. Hence, the PPF is intimately associated with many important adjacent spaces and is an important area for review in the staging and follow-up imaging of head and neck malignancies.

Identification of disease in the PPF has serious treatment and prognostic implications (1, 2, 4). Often, it signifies the presence of perineural spread in the absence of a gross, local, destructive neoplasm. As in a head and neck malignancy at first presentation, the treatment approach to recurrent tumor involving the PPF may be altered to include a wider resection or nonresectability and expansion of the radiation portal. The 5-year survival rate of patients with sinonasal malignancies and invasion of the PPF is dismal (4, 5). Not infrequently, perineural spread in the PPF also portends tumor recurrence and reduced survival (1).

CT and MR imaging are both excellent for follow-up of head and neck malignancies after treatment. With its multiplanar capabilities and superior tissue contrast resolution, however, MR imaging has the advantage over CT in revealing early perineural disease. With the growing use of MR imaging for follow-up of head and neck tumors, the radiologist needs to be familiar with the postoperative appearance of the PPF to distinguish it from recurrent/residual tumor or perineural disease.

On MR images, the normal PPF is seen as a small fatty ''cleft'' lying between the posterior bony wall of the maxillary sinus and the pterygoid plates. It is best identified on axial T1-weighted images because of the presence of hyperintense fat, considering that its thin cortical bony walls are less easily defined on MR images. It is usually bilaterally symmetric and contains tiny flow voids from branches of the internal maxillary artery. There may be mild normal enhancement within after the administration of contrast material because of the presence of small emissary veins (1, 12, 13).

Imaging evidence of disease by local extension or perineural spread in the PPF includes replacement of normal fat signal intensity on T1-weighted MR images and abnormal enhancement or widening of the PPF (1, 2, 7–11). Clearly, the postoperative MR appearance in our cohort mimics that of

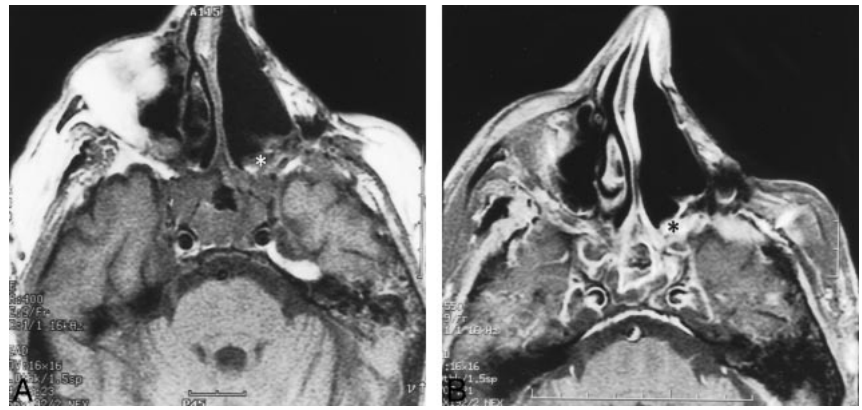

FIG 2. Axial MR images of a 70-year-old man, obtained 55 months after radical maxillectomy for squamous cell carcinoma in the left maxillary sinus.

A and *B,* Corresponding pre- (400/9/2) (*A*) and postcontrast fat-suppressed (*B*) T1-weighted images show persistent replacement of normal fat signal in the left PPF by soft-tissue thickening (*asterisk*) that is slightly hyperintense to muscle and enhances excessively (*B*).

disease. These changes were presumed to be related to granulation tissue and grafting material (such as a myocutaneous flap) in some cases. This abnormal appearance of the postoperative PPF persisted in all patients and lasted up to a maximum of 79 months in our series. Ignorance of this ''normal'' postoperative appearance of the disease-free PPF serves as a potential factor in misdiagnosis.

The PPF space is commonly disrupted during surgical extirpation of large or posteriorly situated maxillary sinus malignancies via approaches such as a radical or extended total maxillectomy, maxillectomy with orbital exenteration, or infratemporal fossa resection. Medial maxillectomies or palatectomies do not usually violate this space. During a standard maxillectomy procedure, it is desirable to remove the posterior maxillary sinus wall as the posterior margin. This is usually the final step performed to detach the specimen because of the close proximity of the internal maxillary artery and potential for significant bleeding. After transecting the pterygoid muscles and exposing the pterygoid plates, the maxilla is down-fractured and detached from the skull by placing a curved osteotome in the PPF or on the pterygoid plates. The remaining soft-tissue attachments are transected with heavy scissors, and the specimen is removed. Any hemorrhage from the maxillary artery or pterygoid venous plexus is controlled by means of surgical clips or suture ligatures. A skin graft is placed over the cheek flap and the remaining posterior soft tissue and is temporarily held in position with packing and a surgical obturator. In some cases, the surgical defect is filled with a myocutaneous free flap (6).

The role of radiation and chemotherapy is not thought to be significant in contributing to the abnormal MR imaging appearance of the PPF after surgical violation in our patients, because five patients had a normal PPF on MR scans obtained after adjunct radiation or chemotherapy or both and before surgery. Furthermore, we are unaware of any literature suggesting that radiotherapy alters the appearance of the PPF.

We presume that in the absence of tumor recurrence, the MR imaging findings in the postoperative PPF represent scar. Unfortunately, in our experience, we found it difficult to distinguish the postoperative PPF from disease involvement reliably on a single MR scan. Nevertheless, obtaining an early postoperative baseline scan, serial imaging to look for stability of findings of the PPF, and absence of new local mass lesion or adjacent perineural spread along the second division of the ipsilateral trigeminal nerve are useful radiologic tools. Clinically, the postoperative PPF may be accessible for examination, and communication with our surgical colleagues is often helpful.

Conclusion

The postoperative PPF always appears abnormal on MR images, even in the absence of disease. This finding probably continues indefinitely and is a potential diagnostic pitfall that requires serial scanning and familiarity with its appearance to avoid misdiagnosis.

References

1. Ginsberg LE. **Imaging of perineural tumor spread in head and neck cancer.** *Semin Ultrasound CT MR* 1999;20:175–186
2. Curtin HD, Williams R, Johnson J. **CT of perineural tumor extension: pterygopalatine fossa.** *AJNR Am J Neuroradiol* 1984;5: 731–737
3. Curtin HD, Williams R. **Computed tomographic anatomy of the pterygopalatine fossa.** *Radiographics* 1985;5:429–440
4. Goepfert H, Dichtel WJ, Medina JE, Lindberg RD, Luna MD. **Perineural invasion of squamous cell skin carcinoma of the head and neck.** *Am J Surg* 1984;148:542–547
5. Gullane PJ, Conley J. **Carcinoma of the maxillary sinus: a correlation of the clinical course with orbital involvement, pterygoid erosion or pterygopalatine invasion and cervical metastases.** *J Otolaryngol* 1983;12:141–145
6. Carrau RL, Myers EN. **Neoplasms of the nose and paranasal sinuses.** In: Bailey BJ, Calhoun KH,eds.*Head & Neck Surgery: Otolaryngology*. 2nd ed, vol 2. Philadelphia: Lippincott-Raven; 1998:1457–1469
7. Ginsberg LE, De Monte F. **Imaging of perineural tumor spread from palatal carcinoma.** *AJNR Am J Neuroradiol* 1998;19:1417–1422
8. Ginsberg LE, De Monte F, Gillenwater AM. **Greater superficial petrosal nerve: anatomy and MR findings in perineural tumor spread.** *AJNR Am J Neuroradiol* 1996;17:389–393
9. Parker GD, Harnsberger HR. **Clinical-radiologic issues in perineural tumor spread of malignant disease of the extracranial head and neck.** *Radiographics* 1991;11:383–399

10. Caldemeyer KS, Mathews VP, Righi PD, Smith RR. **Imaging features and clinical significance of perineural spread or extension of head and neck tumors.** *Radiographics* 1998;18:97–110
11. Ginsberg LE, De Monte F. **Palatal adenoid cystic carcinoma presenting as perineural spread to the cavernous sinus.** *Skull Base Surg* 1998;8:39–43
12. Chong VF, Fan YF. **Pterygopalatine fossa and maxillary nerve infiltration in nasopharyngeal carcinoma.** *Head Neck* 1997;19: 121–125
13. Chong VF, Fan YF, Khoo JB, Lim TA. **Comparing computed tomographic and magnetic resonance imaging visualisation of the pterygopalatine fossa in nasopharyngeal carcinoma.** *Ann Acad Med Singapore* 1995;24:436–441
14. Daniels DL, Mark LP, Ulmer JL, et al. **Anatomic moment: osseus anatomy of the pterygopalatine fossa.** *AJNR Am J Neuroradiol* 1998;19:1423–1432
15. Soames RW. **Skeletal system.** In: Bannister LH, Berry MM, Collins P, Dyson M, Dussek JE, Ferguson MWJ, eds. *Gray's Anatomy.* 38th ed. Churchill Livingstone;1995:561–562
16. Daniels DL, Rauschning W, Lovas J, Williams AL, Haughton VM. **Pterygopalatine fossa: computed tomographic studies.** *Radiology* 1983;149:511–516